SUPPLEMENTARY MATERIAL:
Nanocluster Formation Process in Peptide Solutions: Dynamics and Bioactivity Implications

Dimitar Kaynarov[a], Karina Marinova[a], Rossitsa Marinova[b,*], Peicho Petkov[b], Lyudmila Velkova[a,*], Aleksandar Dolashki[a], Petar Petrov[a], Leandar Litov[b], Elena Lilkova[c], Nevena Ilieva[c], Pavlina Dolashka[a]

[a]*Institute of Organic Chemistry with Centre of Phytochemistry at the Bulgarian Academy of Sciences, Acad. G. Bonchev Str., Block 9, Sofia, 1113, , Bulgaria*
[b]*Sofia University "St. Kl. Ohridsky", Physics Faculty, 5, James Bourchier Blvd, Sofia, 1164, , Bulgaria*
[c]*Institute of Information and Communication Technologies at the Bulgarian Academy of Sciences, Acad. G. Bonchev Str., Block 2, Sofia, 1113, , Bulgaria*

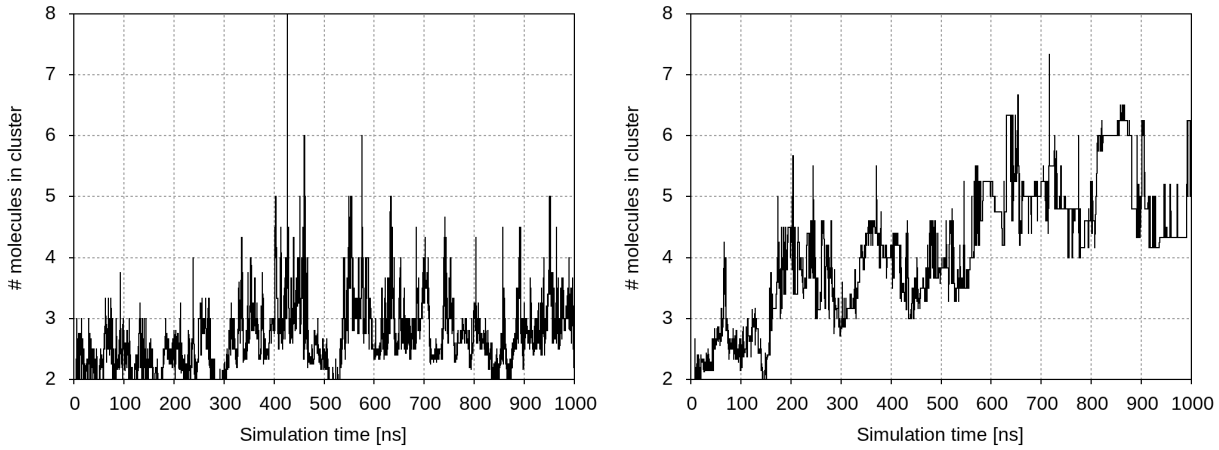

(a) (b)

Figure S1: The average cluster size in the (a) p1, resp. (b) p3 mono-component solutions at a concentration of 10 mg/mL.

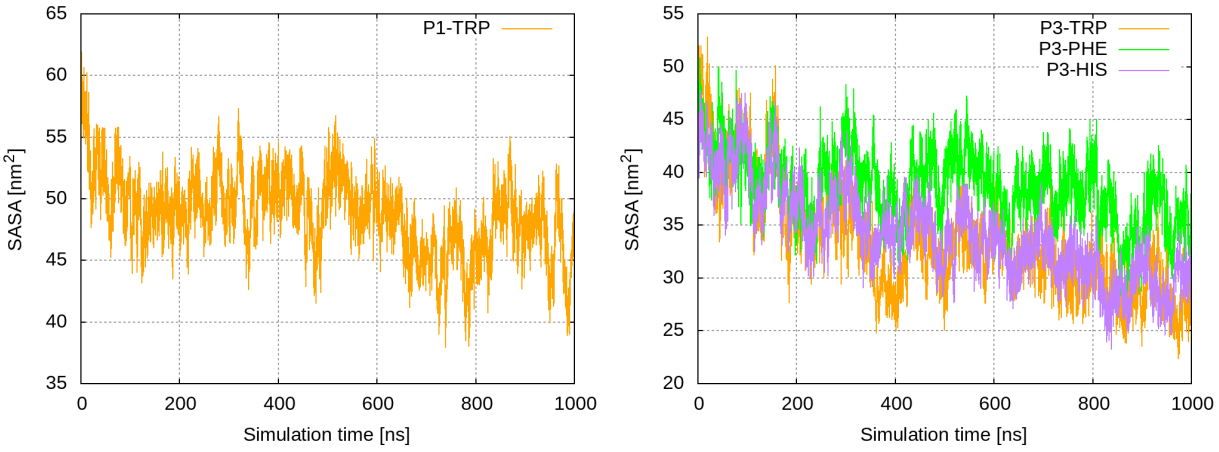

(a) (b)

Figure S2: SASA of the aromatic residues in the (a) p1, resp. (b) p3 mono-component solutions at a concentration of 10 mg/mL.

*Corresponding author
Email addresses: rosie.marinova@gmail.com (Rossitsa Marinova), Lyudmila.Velkova@orgchm.bas.bg (Lyudmila Velkova)

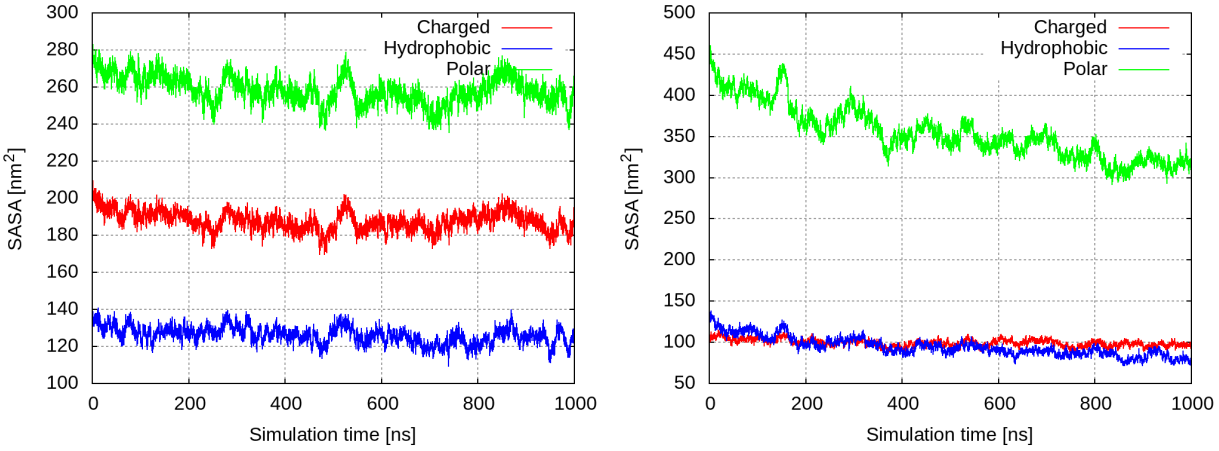

(a) (b)

Figure S3: SASA of the hydropbic (blue), polar (green), and charged (red) residues in the (a) p1, resp. (b) p3 mono-component solutions at a concentration of 10 mg/mL.

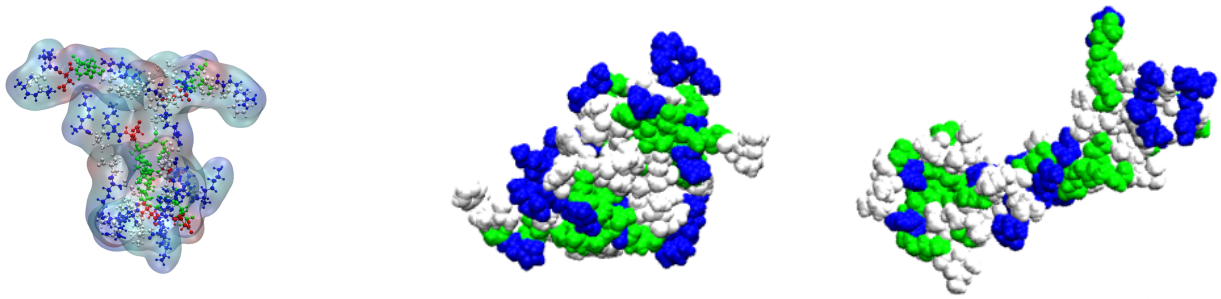

(a) (b)

Figure S4: The largest clusters in the (a) p1 and (b) p3 monocomponent solutions at a concentration of 10 mg/mL in surface/VdW representation; basic residues are coloured in blue, acidic — in red, polar — in green, and non-polar — in white.

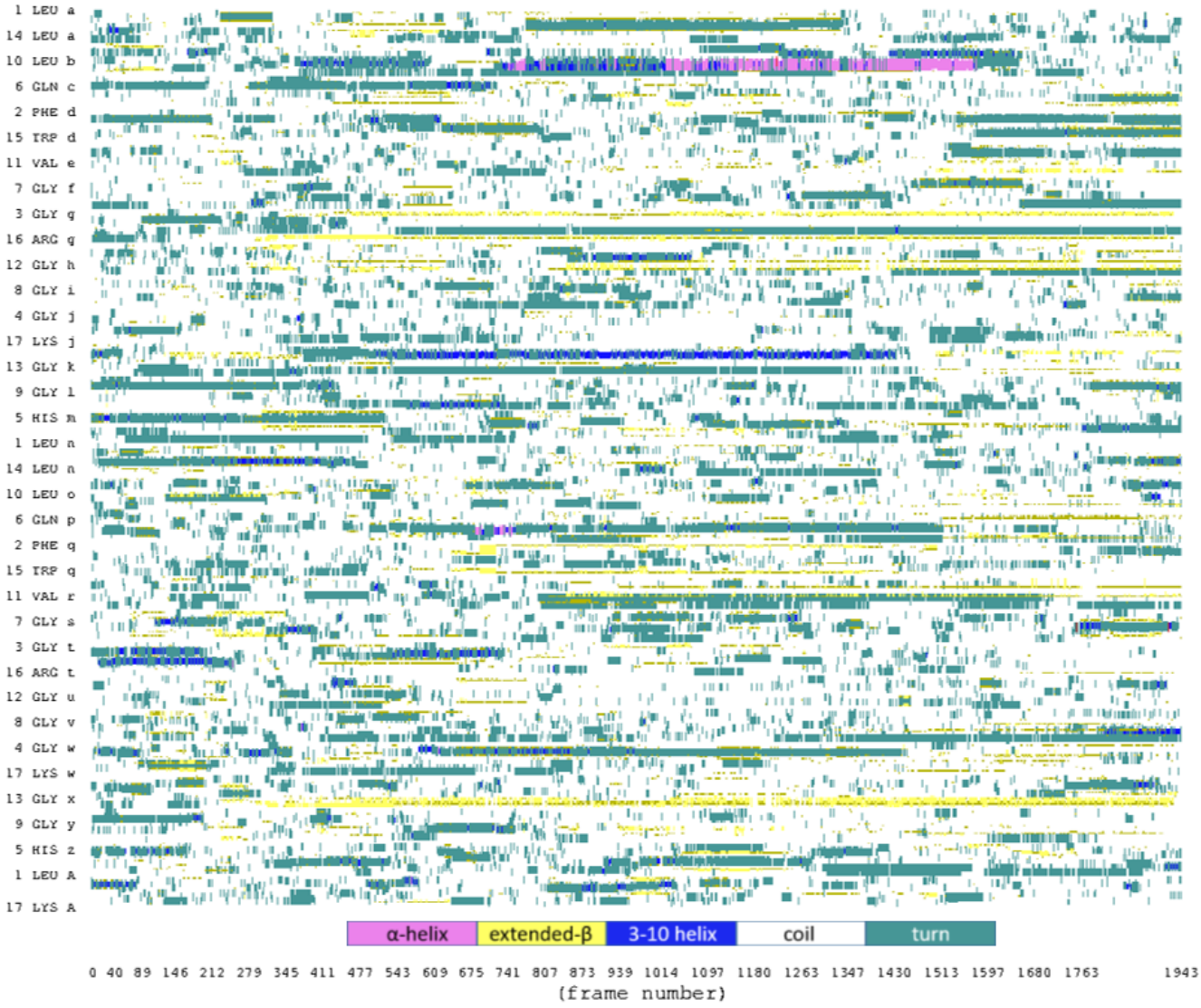

Figure S5: Evolution of the secondary structure of the p3 monocomponent solution.

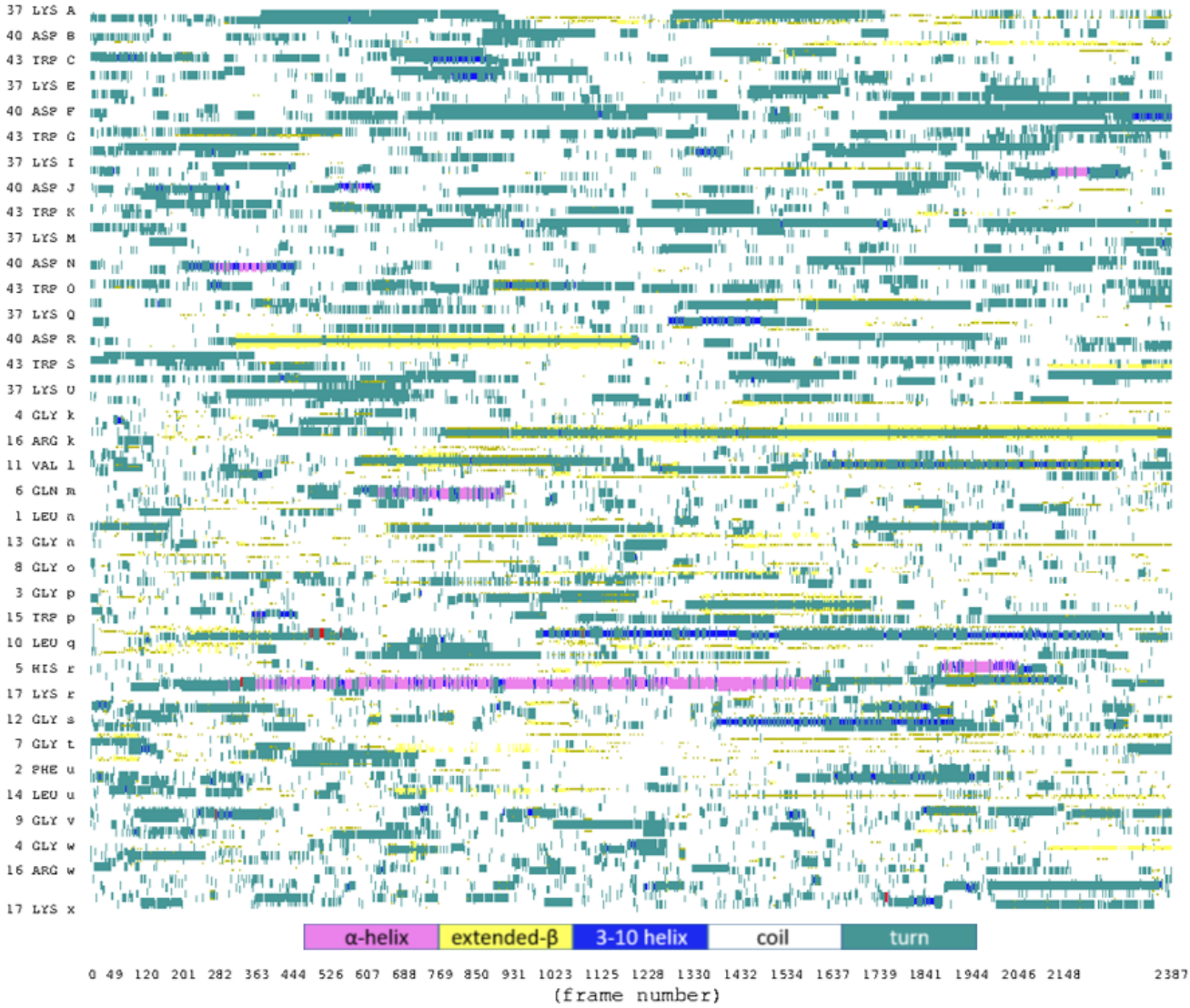

Figure S6: Evolution of the secondary structure of the p1+p3 multicomponent solution.

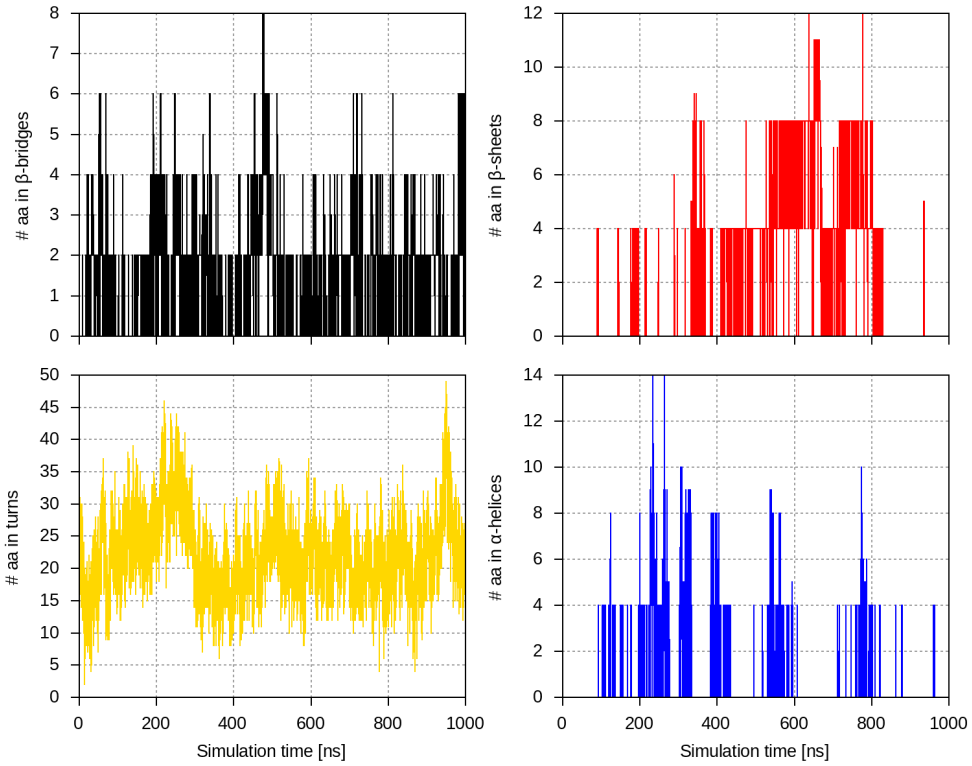

Figure S7: Number of residues involved in the four main secondary-structure elements in the p1 solution.

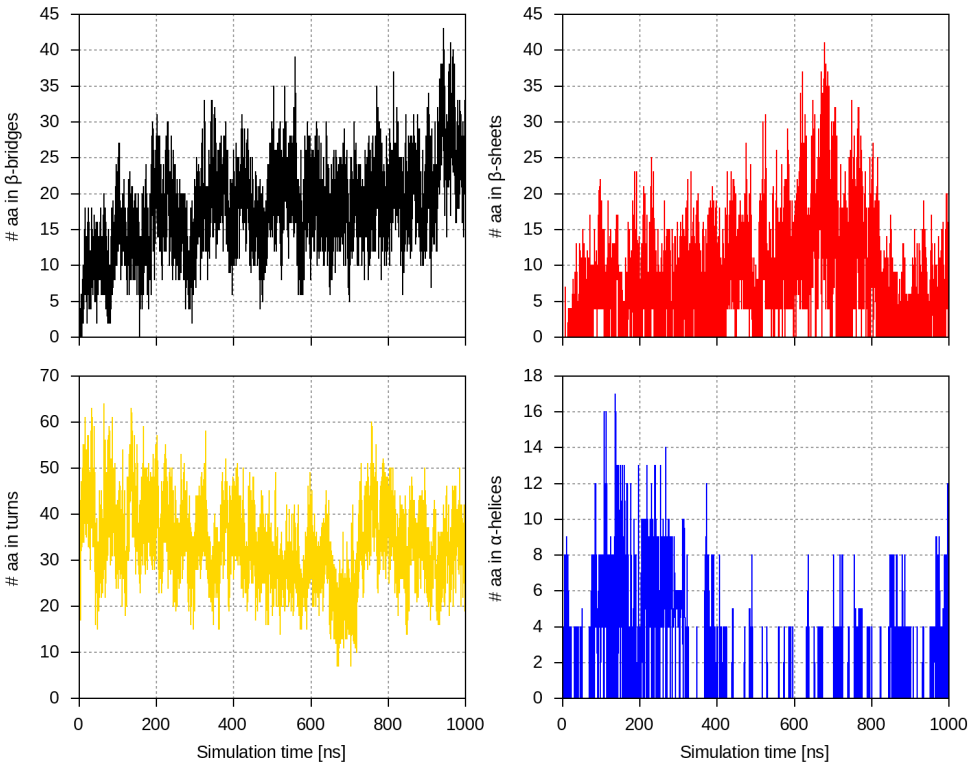

Figure S8: Number of residues involved in the four main secondary-structure elements in the p3 solution.

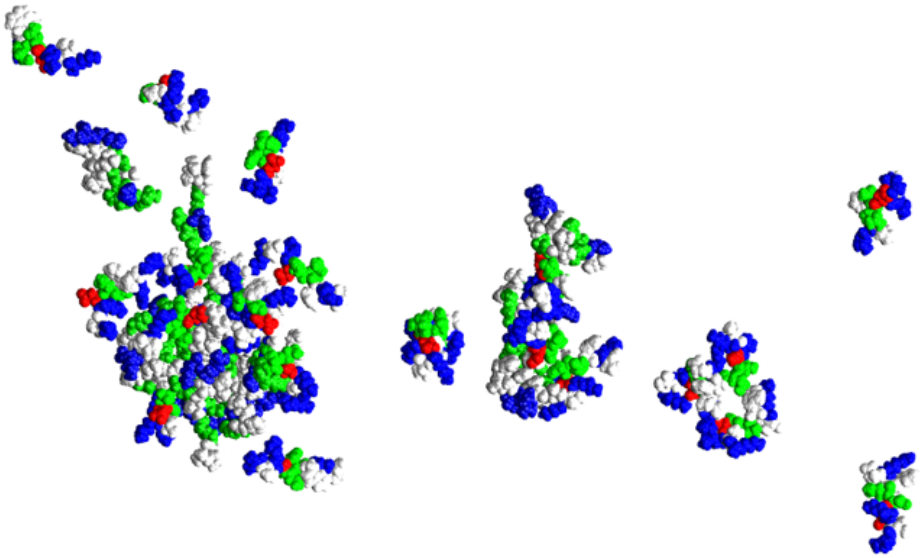

Figure S9: Final conformation (clusters formed) by the end of the multicomponent simulation.

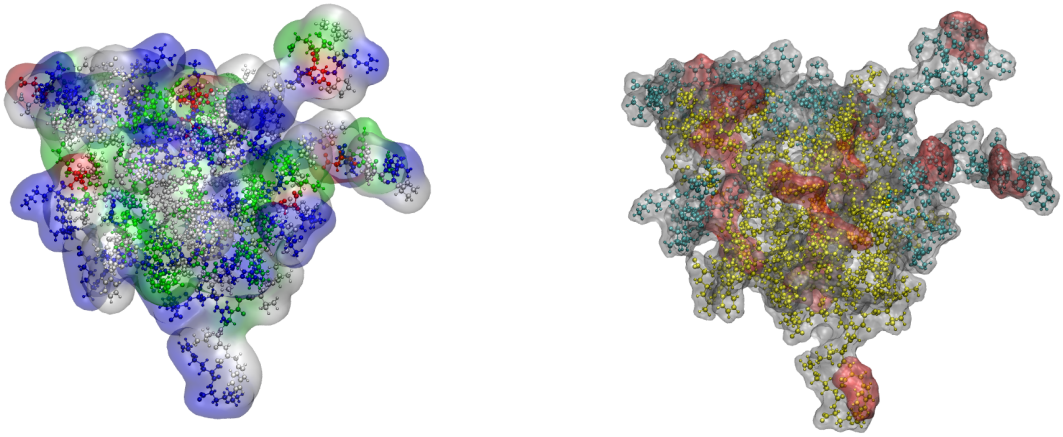

(a) (b)

Figure S10: The largest cluster in the multi-component p1+p3 simulation, in surface representation: (a) coloured by residue type, basic residues in blue, acidic – in red, polar – in green, non-polar – in white; (b) coloured by peptide type, p1 in blue, p3 in yellow, Trp residues highlighted in red.

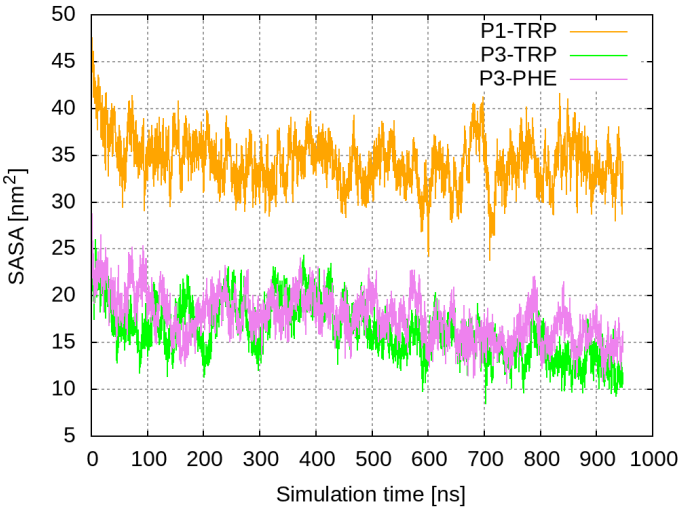

Figure S11: SASA of the Trp and Phe residues in the multicomponent solution.

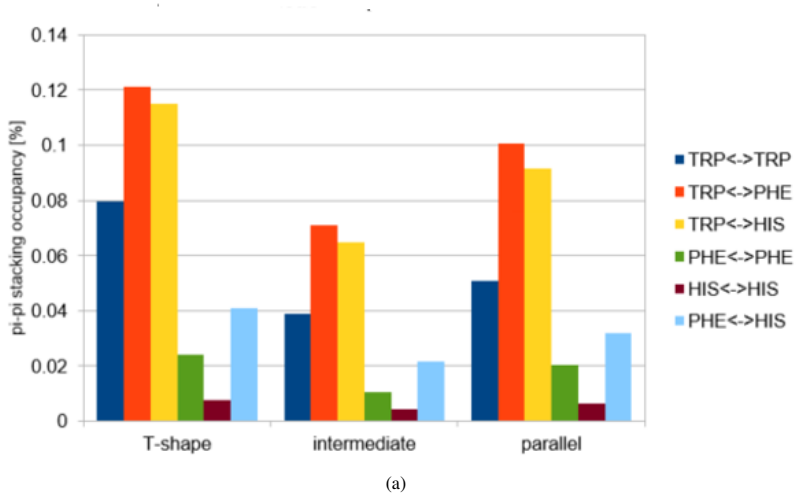

(a)

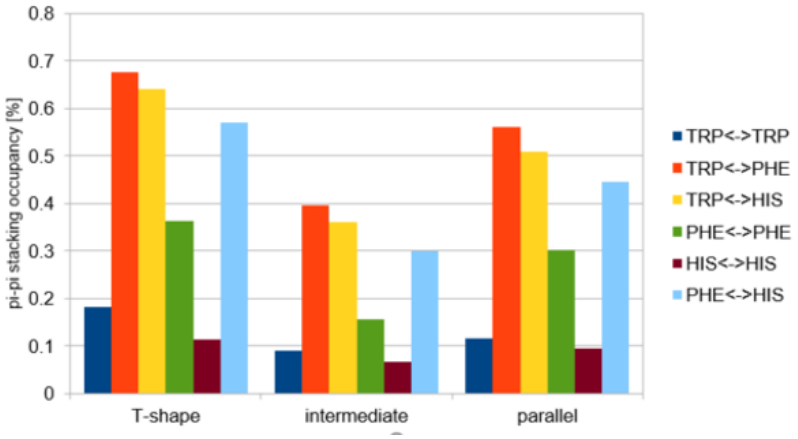

(b)

Figure S12: Percentage of the π-π stacking conformations in the peptide mixture simulation: (a) by kind per aromatic pairs; (b) by kind per amino acid type pairs.

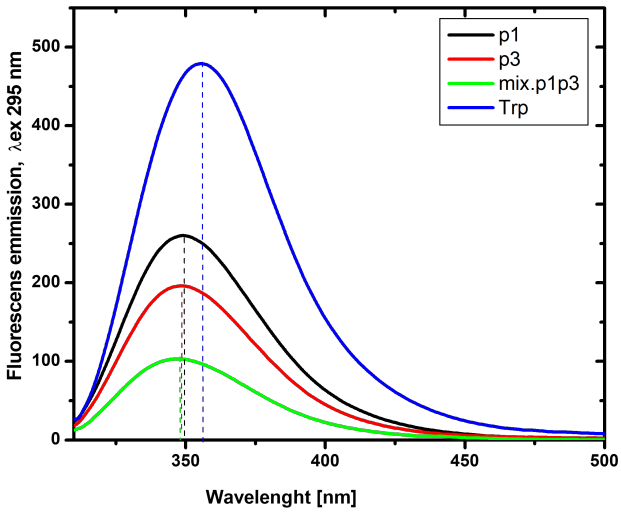

Figure S13: Fluorescence emission spectra of p1, p3, and p1+p3 compared to hydrophobic amino acid tryptophan (concentration of 10 mg/mL) at λ_{ex} = 295 nm immediately after the digestion of the peptides in a phosphate buffer (asymmetric quartz cuvette with 4/10 mm optical length at 22°C).

Table S1: Inhibition of *B. subtilis* growth by p1, p3, (p1+p3) combination, and bombinin at different concentrations.

Concentration	p1		p3		p1+p3		bombinin	
[mg/ml]	Inhibition [%]	Std. Dev.	Inhibition [%]	Std. Dev.	Inhibition [%]	Std. Dev.	Inhibition [%]	Std. Dev.
11.4	63.3	4.2	100.0	3.5	100.0	3.2	100.0	4.2
5.7	55.0	3.0	100.0	4.6	100.0	4.1	100.0	4.3
2.8	52.8	3.9	100.0	3.5	100.0	3.3	99.0	5.5
1.4	54.7	4.8	100.0	4.8	100.0	2.5	86.8	4.7
0.7	50.1	3.8	99.5	4.7	79.0	5.2	68.1	6.1
0.4	47.2	3.4	77.4	4.4	33.8	3.4	37.1	3.0
0.2	38.6	3.3	45.6	3.2	28.5	3.3	34.4	6.3
0.1	30.8	3.8	47.4	3.8	22.9	4.1	22.6	5.5

Table S2: Inhibition of *E. coli* 3458 growth by p1, p3, (p1+p3) combination, and bombinin at different concentrations.

Concentration	p1		p3		p1+p3		bombinin	
[mg/ml]	Inhibition [%]	Std. Dev.	Inhibition [%]	Std. Dev.	Inhibition [%]	Std. Dev.	Inhibition [%]	Std. Dev.
11.4	100.0	4.2	100.0	3.2	96.6	3.3	100.0	3.2
5.7	49.5	6.7	100.0	3.4	100.0	4.4	100.0	4.4
2.8	53.6	3.0	100.0	3.3	100.0	3.8	100.0	4.3
1.4	33.8	3.8	100.0	4.2	100.0	3.4	85.9	4.2
0.7	34.8	3.8	99.3	3.3	54.6	5.8	42.9	3.3
0.4	42.8	4.3	57.0	5.4	35.1	5.0	18.4	6.4
0.2	28.0	4.4	55.0	3.2	39.3	4.3	60.8	3.2
0.1	30.9	5.5	45.7	4.6	54.8	5.8	47.9	3.6